**SANDIA REPORT**
SAND2004–0414
Unlimited Release
Printed March 2004

# *In situ* clay formation: Evaluation of a proposed new technology for stable containment barriers

J. T. Fredrich, A. A. DiGiovanni, and K. L. Nagy

Prepared by
Sandia National Laboratories
Albuquerque, New Mexico 87185 and Livermore, California 94550

Sandia is a multiprogram laboratory operated by Sandia Corporation,
a Lockheed Martin Company, for the United States Department of
Energy under Contract DE-AC04-94AL85000.

Approved for public release; further dissemination unlimited.

Sandia National Laboratories

Issued by Sandia National Laboratories, operated for the United States Department of Energy by Sandia Corporation.

**NOTICE:** This report was prepared as an account of work sponsored by an agency of the United States Government. Neither the United States Government nor any agency thereof, nor any of their employees, nor any of their contractors, subcontractors, or their employees, makes any warranty, express or implied, or assumes any legal liability or responsibility for the accuracy, completeness, or usefulness of any information, apparatus, product, or process disclosed, or represents that its use would not infringe privately owned rights. Reference herein to any specific commercial product, process, or service by trade name, trademark, manufacturer, or otherwise, does not necessarily constitute or imply its endorsement, recommendation, or favoring by the United States Government, any agency thereof, or any of their contractors or subcontractors. The views and opinions expressed herein do not necessarily state or reflect those of the United States Government, any agency thereof, or any of their contractors.

Printed in the United States of America. This report has been reproduced directly from the best available copy.

Available to DOE and DOE contractors from
Office of Scientific and Technical Information
P.O. Box 62
Oak Ridge, TN 37831

Prices available from (615) 576-8401, FTS 626-8401

Available to the public from
National Technical Information Service
U.S. Department of Commerce
5285 Port Royal Rd
Springfield, VA 22161

NTIS price codes
Printed copy: A03
Microfiche copy: A01

SAND2004-0414
Unlimited Release
Printed March 2004

# *In situ* Clay Formation: Evaluation of a Proposed New Technology for Stable Containment Barriers

J. T. Fredrich and A. A. DiGiovanni
Geophysical Technology Department
Sandia National Laboratories
P.O. Box 5800
Albuquerque, NM 87185-0750

K. L. Nagy
Department of Earth and Environmental Sciences
University of Illinois at Chicago
Chicago, IL 60607-7059

## Abstract

Containment of chemical wastes in near-surface and repository environments is accomplished by designing engineered barriers to fluid flow. Containment barrier technologies such as clay liners, soil/bentonite slurry walls, soil/plastic walls, artificially grouted sediments and soils, and colloidal gelling materials are intended to stop fluid transport and prevent plume migration. However, despite their effectiveness in the short-term, all of these barriers exhibit geochemical or geomechanical instability over the long-term resulting in degradation of the barrier and its ability to contain waste. No technologically practical or economically affordable technologies or methods exist at present for accomplishing total remediation, contaminant removal, or destruction-degradation *in situ*. A new type of containment barrier with a potentially broad range of environmental stability and longevity could result in significant cost-savings. This report documents a research program designed to establish the viability of a proposed new type of containment barrier derived from *in situ* precipitation of clays in the pore space of contaminated soils or sediments. The concept builds upon technologies that exist for colloidal or gel stabilization. Clays have the advantages of being geologically compatible with the near-surface environment and naturally sorptive for a range of contaminants, and further, the precipitation of clays could result in reduced permeability and hydraulic conductivity, and increased mechanical stability through cementation of soil particles. While limited success was achieved under certain controlled laboratory conditions, the results did not warrant continuation to the field stage for multiple reasons, and the research program was thus concluded with Phase 2.

This page intentionally left blank.

# Preface

This report summarizes project CU-1093 "In-Situ Clay Formation: A New Technology for Stable Containment Barriers," performed under sponsorship of the Strategic Environmental Research and Development Program (SERDP), the Department of Defense's (DoD) corporate environmental research and development (R&D) program, planned and executed in full partnership with the Department of Energy (DOE) and the Environmental Protection Agency (EPA).

The concept that was the subject of the research effort was originally described in a proposal written by K. L. Nagy, J. D. Betsill, and J. T. Fredrich (all Sandia), and recommended for funding in FY98. The results of Phase 1 gel experiments are reported in three papers published in the open literature by K. L. Nagy (currently at University of Illinois at Chicago) and co-workers. This report describes the results of the Phase 2 laboratory experiments that were aimed at precipitating clay phases in sediments. The laboratory experiments were performed as a collaborative effort with Professor Nagy, then at the University of Colorado, Boulder. In 2001, Fredrich and Nagy concluded that the results of the Phase 2 laboratory experiments did not warrant continuation of the research.

This page intentionally left blank.

## Table of Contents

Abstract ..... 3
Preface ..... 5
Table of Contents ..... 7
Figures ..... 9
Tables ..... 11
1 Introduction ..... 13
2 The Concept ..... 14
3 Overview of the Research Project ..... 16
4 Phase 2 Laboratory Experiments ..... 17
4.1 Experiments to evaluate *in situ* mesoporous silicate precipitation ..... 20
4.1.1 Solution preparation and column mixing ..... 20
4.1.2 Results ..... 20
4.2 Experiments to evaluate *in situ* layered double hydroxide precipitation ..... 23
4.2.1 Solution preparation and column mixing ..... 24
4.2.2 Results ..... 25
4.3 Microanalysis ..... 26
5 Summary ..... 19
6 References ..... 32

This page intentionally left blank.

## Figures

**Figure 4.1** Experimental setup for column mixing experiments and permeability testing. A plastic beaker below the column collects solutions that exit the column. ..... 18
**Figure 4.2** Falling head permeameter testing configuration (after Dullien, 1992). ..... 19
**Figure 4.3** Backscattered electron micrographs showing the bimodal morphology of Arizona magic sand. Grains are smooth and faceted (top), or alternatively rough and irregular (bottom). ..... 21
**Figure 4.4** Bulk sample following in situ precipitation of MPS in sand pack (Arizona magic sand), followed by drying at 60 °C after removal from the column. Indurated material taken from the lower portion of the plastic syringe is located at the left side of the image and mimics the cone shape of the syringe bottom. The larger piece to the right of the image is from the column head where solutions were introduced. The smaller pieces in the center and the loose sand came from space in between the two ends (sample from experiment AZ-MPS-11, Table 4.2). ..... 23
**Figure 4.5** Bulk sample following in situ precipitation of LDH in sand pack (Arizona magic sand), followed by drying at 60 °C after removal from the column. Compared to the experiments with mesoporous silicate precipitation (see Figure 4.4), the indurated regions of the LDH sand packs were smaller and noticeably more friable. Material from the lower region of the column is shown on the left and upper region at the right of the image (sample from experiment AZ-7, Table 4.2). ..... 26
**Figure 4.6** (Top) A low magnification back scattered electron micrograph of an indurated region of a MPS sand pack after drying at 60 °C. The sand pack appears unchanged from the starting material, and the cohesion following the experiment suggests the presence of a very thin coating of MPS precipitate. (Middle) A "neck" of MPS precipitate can be observed between two sand grains (boxed region). (Bottom) A higher magnification view of the MPS precipitate bridging the two grains shown in the middle micrograph. (Sample from experiment AZ-MPS-11.) . ..... 16
**Figure 4.7** (Top) A low magnification back scattered electron micrograph of an indurated region of an LDH sand pack after drying at 60 °C. (Middle) The LDH precipitate is clearly evident as a coating over grains (right) where platelet size is a few microns, and partially filling the pore space where sub-micron platelets dominate (left). Despite the pervasiveness of the coating, the strength of the bonded LDH sand packs is less than that of the MPS sand packs. (Lower) The rose-like morphology of the LDH precipitate partially filling previously open pore space (left middle) is very well developed. The typical size of the platelets is 500 nm. (Sample from experiment AZ-7.) ..... 17
**Figure 4.8** Spectra collected from powdered region from LDH precipitation experiment AZ-7. A light gold-palladium film coats all samples as required in scanning electron microscopy. (Top) The signal for Mg and Al is moderate as are the Au-Pd peaks. (Middle) The Mg/Al signal from these two regions is minimal, indicating possible lack of coverage or incomplete formation of LDH. (Bottom) The signal here is strong and in the proper ratio (2:1) of the precursor solutions. The presence of the chlorine peak suggests that this area contains remnants of the unreacted precursor solution..... 30

This page intentionally left blank.

## Tables

**Table 4.1** Summary of *in situ* precipitation of mesoporous silicate (MPS) in sand pack experiments. ..... 22
**Table 4.2** Summary of *in situ* precipitation of layered double hydroxide (LDH) in sand pack experiments. ..... 25

This page intentionally left blank.

# 1 Introduction

Containment of chemical wastes in near-surface and repository environments is accomplished by designing engineered barriers to fluid flow. Impermeable barriers are intended to contain wastes for subsequent cleanup treatment or for longer-term isolation in cases where no effective cleanup treatment yet exists. Impermeable barriers also have recently been applied as components of "funnel and gate" approaches to selectively channel contaminated fluid flow through a reactive treatment zone (*Shoemaker et al*., 1996). Containment barrier technologies such as clay liners, soil/bentonite slurry walls, soil/plastic walls, artificially grouted sediments and soils, and colloidal gelling materials are intended to stop fluid transport and prevent plume migration. However, despite their effectiveness in the short-term, all of these barriers will exhibit geochemical or geomechanical instability over the long-term resulting in degradation of the barrier and its ability to contain waste. For example, grouts and colloidal silica both require saturated conditions to maintain their structural integrity (*Rumer and Ryan*, 1995; *Whang*, 1996). No technologically practical or economically affordable technologies or methods exist at the present time for accomplishing total remediation, contaminant removal, or destruction-degradation *in situ*.

A new type of containment barrier with a potentially broader range of environmental stability and longevity could result in significant cost-savings to the Department of Defense (DoD) and Department of Energy (DOE). This report documents a research effort designed to establish the viability of a proposed new type of containment barrier derived from the *in situ* precipitation of clays in the pore space of contaminated soils or sediments. The concept builds upon technologies that exist for colloidal or gel stabilization. Unlike colloidal or gel barriers, however, a precipitated-clay barrier would not require saturated conditions to be functional. Thus, it could be emplaced without loss of performance in the vadose zone as well as in areas with fluctuating water tables. Clays have the advantages of being geologically compatible with the near-surface environment and naturally sorptive for a range of contaminants. The precipitation of clays *in situ* in soils and sediments could result in reduced permeability and hydraulic conductivity, and increased mechanical stability through cementation of soil particles. By analogy with diagenesis in sedimentary rocks, it may be possible to engineer "artificial" lithification in soils and sediments. Unlike natural diagenesis, however, the time-scale for clay growth would be accelerated greatly from more than tens of thousands of years down to a few weeks.

The research effort described in this report was conducted under project CU-1093 "In-Situ Clay Formation: A New Technology for Stable Containment Barriers," performed under sponsorship of the Strategic Environmental Research and Development Program (SERDP), the DoD's corporate environmental research and development (R&D) program, planned and executed in full partnership with the DOE and the Environmental Protection Agency (EPA). The project was funded in FY98, FY99, and FY00. The project was concluded following Phase 1 and Phase 2 laboratory testing that indicated that the technology would not be practical to implement in the desired field settings.

# 2 The Concept

Functional subsurface barriers are designed to achieve one of two desired outcomes. The first is removal of the contaminant as the groundwater flows through a reactive barrier. The second is prevention of plume migration past an impermeable barrier. Materials in the forefront for use in reactive barriers include zero-valent metals, especially Fe, that reduce and adsorb toxic metals such as Cr(VI) (*EPA*, 1995). Other materials, including lime, fly ash, Fe-oxyhydroxides, calcium phosphate, Fe-sulfate, and surfactant-coated zeolites have also been shown to sorb various contaminants to differing degrees under prescribed environmental conditions (*EPA*, 1995; *Davidovits*, 1993; *Bowman et al*., 1995). While many of these materials have narrow windows of geochemical stability that may or may not be found in nature, fewer exhibit any geomechanical stability. The latter is particularly important because compaction can produce fractures, and therefore, preferential flowpaths that bypass most of the surface area of the reactive material, effectively diminishing its utility. Thus, there is a need for development of a new containment barrier that will be geochemically stable in a wide range of natural contaminated environments and that will be geomechanically stable over the long term, in particular for the time period required by performance assessment.

When designing a barrier material, existing soil, sediment, or rock often is excluded from consideration. In reality, the pre-existing natural material can form the backbone of the engineered barrier. Deep-soil mixing and jet grouting (*Rumer and Ryan*, 1995; *Evans*, 1996; *Filz and Mitchell*, 1996) are two relatively recent techniques used in constructing vertical barrier walls that take advantage of the natural soil in constructing the barrier. Although these two techniques destroy the natural arrangement of soil particles, the inclusion of soil as part of the barrier is similar conceptually to what happens during lithification. Permeation grouting (*Rumer and Ryan*, 1995) is a more established process for barrier construction that is similar to the natural mechanical and geochemical processes that cement together individual mineral grains to form a rock. Depending on the grain size of primary phases and the amount and location of secondary cementing phases, the porosity and permeability of a rock can be quite variable. Given that permeability is the single rock property that controls fluid flow, engineering *in situ* the production of materials that reduce permeability is preferred. Ideally, the material that reduces permeability, or hydraulic conductivity, should also enhance chemical retardation.

The class of minerals that will have the greatest effect on permeability for the smallest volume precipitated is sheet silicates or layered-clay phases (hereafter called “clays”). In natural lithification, clays form small thin grains that tend to be randomly oriented, thus greatly increasing the tortuosity of flowpaths. In addition, they tend to nucleate at pore throats, the “weak links” in the flow pathways. The requirement of geochemical stability is also satisfied by sheet silicates. In nature, they grow as stable minerals at ambient and near-ambient conditions and have excellent sorption characteristics for cations and cationic molecules. By virtue of their nucleation and growth at pore throats, clays may also be effective in retarding migration of organic contaminants such as DNAPLs. Expandable clays such as smectites can also adsorb organics within their interlayers (*Raussell-Colom and Serratosa*, 1987; *Johnston*, 1996). Minerals of similar layer structure called

hydrotalcites show strong sorption affinities for anions. Although the stability limits of hydrotalcites are not well known, their structural similarity to clays suggests they could precipitate and reduce permeability by similar mechanisms.

Injection of Portland cement-based grouts directly into natural materials has been applied (*Davidovits*, 1993; *Evans*, 1996; *Filz and Mitchell*, 1996) as an impermeable barrier design. Grouts can show significant geochemical instability in the natural environment. In time, common groundwater components such as $SO_4^{2-}$, $CO_3^{2-}$, and $Mg^{2+}$, if present in sufficient concentration, can degrade grout. This geochemical instability can lead to geomechanical instability such as fracture formation. Also, the processes of jet grouting and deep-soil mixing can disrupt any pre-existing structure that would enhance mechanical endurance.

Barriers derived from gelling technology have been used both in the petroleum and environmental remediation industries. Mineral polymer gels have been used successfully to plug flow from water-producing zones in oil wells and inorganic gels are used for consolidating weak formations and plugging lost circulation (*Borling et al*., 1994). *Borling et al.* reported that Si-gels have been used since the 1920s, but that problems arise in controlling their relatively fast gelation times. Schlumberger-Dowell holds a patent on an inorganic Al-gel system applied to stop water flow in oil wells (*Parker and Davidson*, 1989). This gel contains urea which when heated at downhole temperatures increases the pH (by an increase in the pK of the acid dissociation constant) to a region where metastable Al-polymeric materials precipitate. One advantage of this system is that injection is accomplished with a fluid that has a viscosity near that of water before gelation as opposed to higher viscosities of the polymer gels. This allows deeper penetration of the gel into the formation to obtain a greater effect on permeability. A second advantage is that the conditions and rates of gelation can be controlled. This technology is used in day-to-day operations and is effective, at least for the typical lifetime of a producing well. Disadvantages are that the aluminum phases that form from the gels are metastable and can dehydrate or recrystallize over long periods of time.

DuPont (*Whang*, 1996) has investigated the construction of containment barriers using injected colloidal silica. Their technologies include surface chemical modification of the colloidal silica to control gellation time. A significant disadvantage of this technology is that if the gel dehydrates, it can crack creating fast flow paths for contaminant transport. This limits its application to highly saturated soil environments and consequently areas of wetter climate.

Another *in situ* precipitation process, again proposed by DuPont (*Whang*, 1996), involves injection of mildly acidic (pH = 3) Fe solutions in which high concentrations of Fe are maintained by an organic chelating agent. The solutions also contain a urea/urease mixture. The urease breaks down the urea which generates ammonia raising the pH and causing Fe-hydroxides to precipitate. In this example, the Fe-hydroxides have the added advantage of having high sorption affinity for a variety of chemical wastes including metals and organics. DuPont researchers have observed a reduction of hydraulic conductivity from $10^{-2}$ cm/s to $10^{-7}$ cm/s in laboratory sand columns after Fe-hydroxide precipitation by permeation grouting.

The methods used to precipitate simple metal hydroxides and gels used in the environmental remediation and petroleum industries could be extended to the precipitation of sheet aluminosilicate, or clay, minerals. This would provide the added advantages of geochemical and geomechanical stability described above.

In an experiment designed to simulate a natural situation, *Michalopoulos and Aller* (1995) demonstrated that K-Fe-Mg sheet silicates can grow in relatively short times, 12 to 36 months, in delta sediments from the Amazon River incubated under anoxic conditions in the laboratory at 28°C. The clay formation appears to require a fairly mobile form of dissolved Al and is accelerated in the presence of unstable Si glass beads. Results from numerous laboratory syntheses conducted from one to three decades ago show that sheet silicates can be grown from inorganic gels at room temperature in a matter of days to months depending on initial gel composition and pH. However, typically in these older studies, the reported results indicated that the identity of the newly formed clays was poorly known, the yield of crystals was not high, and the crystallinity of the clays was low (i.e., small grain size). In other words, the kinetics of clay formation from the gels were not optimized in these investigations.

Together, the above studies on clay precipitation from gels, clay precipitation in Amazon River delta sediments, and commercial applications of mineral-gels to occlude porosity and reduce permeability, all suggested that the engineering of clay precipitation *in situ* to form impermeable and/or reactive barriers was a feasible goal.

# 3 Overview of the Research Project

The purpose of project CU-1093 "In-Situ Clay Formation: A New Technology for Stable Containment Barriers" was to evaluate the viability of a proposed new type of containment barrier, derived from the *in situ* precipitation of clays in the pore space of contaminated soils or sediments, with a potentially broad range of environmental stability and longevity.

The research program was to be conducted in discrete stages that involved a number of different institutions. The first phase of the research effort focused on the laboratory synthesis of clays and clay-like materials from gels at room or ambient temperature. As a result of K. L. Nagy's move from Sandia to the University of Colorado just prior to the project's start, this effort was conducted at the University of Colorado, with supporting analytic (Transmission Electron Microscopy) work conducted at the University of Wisconsin. The initial effort focused on reproducing experimental designs from various published studies in which clay products were identified (e.g., *Decarreau* 1980, 1981; *Decarreau and Bonnin*, 1986; *Decarreau et al*., 1987; *Flehmig*, 1992; *Harder*, 1971, 1974, 1976, 1977, 1978; *Hem and Lind*, 1974; *La Iglesia Fernandez and Martin Vivaldi*, 1973; *La Iglesia and Martin-Vivaldi*, 1975; *La Iglesia and Sema*, 1974, *Linares and Huertas*, 1971a,b; *Siffert*, 1962; *Siffert and Wey*, 1973). In addition to these formulations, the synthesis of an anionic clay called a layered double hydroxide (*Cavani et al*., 1991), that has a naturally occurring mineral counterpart called a hydrotalcite (e.g., *Taylor and McKenzie*, 1980), was

attempted. A third type of material investigated falls within the new class of mesoporous silica materials that can be formed at room temperature using surfactant templates (e.g., *Kresge et al*., 1992; *Anderson et al*., 1995; *McMullen et al*., 1995). Finally, a related study with researchers at the University of Grenoble was conducted to investigate the nucleation of clays on quartz surfaces under ambient conditions. The results of the Phase 1 research are described in three technical papers published in the peer-reviewed scientific literature (*Manceau et al*., 1999; *Zhao et al*., 2000, *Zhao et al*., in press) and are not described further in this report.

The second phase of the research effort focused on precipitating two of the studied clay and clay-like materials, anionic clay and mesoporous silica, in natural sediments under laboratory conditions. As originally designed, Phase 2 was to be followed by a third phase that included a pilot scale test to be conducted in a physical model, followed by a full-scale field test. The research program included several Go/No Go decision points, and because the results of the Phase 2 experiments indicated that application in the field would not be practical, the research program concluded during Phase 2. As noted, the Phase 1 research is documented in three papers published in the open literature. The Phase 3 research plan was outlined in a white paper submitted to the SERDP project office on August 23, 2000 ("In-Situ Clay Formation: A New Technology for Stable Containment Barriers: Potential for conducting pilot experiments in a physical model", by B.P. Dwyer, J.T. Fredrich, and K.L. Nagy). The remainder of this report describes the results of the Phase 2 research program and rationale for not continuing to the field scale.

# 4 Phase 2 Laboratory Experiments

Following conclusion of the Phase 1 gel experiments, the aim of the Phase 2 laboratory experiments was to precipitate clay and/or clay-like solids *in situ* in both quartz and natural sediments in laboratory sand-column scale experiments. Emplacement of the solutions/gels in the laboratory tests was to emulate field technologies such as permeation and jet grouting, and soil-mixing. The laboratory experiments focused on the optimization of clay gel mixes, gelation/setup time, and hydraulic conductivity reduction.

Success of the method was to be demonstrated by obtaining a significant reduction in permeability (or hydraulic conductivity) and increase in geomechanical stability, under conditions practical for field application. Ultimately, the experiments needed to demonstrate that practical quantities of clays and/or clay-like solids could be formed within a timeframe appropriate for installment of a barrier, and secondly, that the material properties would be improved over those of existing containment barriers.

Clay and clay-like solids were preciptated *in situ* in two different sands, Arizona Magic Sand, a nearly pure quartz sand of 0.1-1 mm grain size, and U.S. Silica Min-U-Sil-10, a crushed sand with average grain size of 10 microns, in plastic syringes in the laboratory

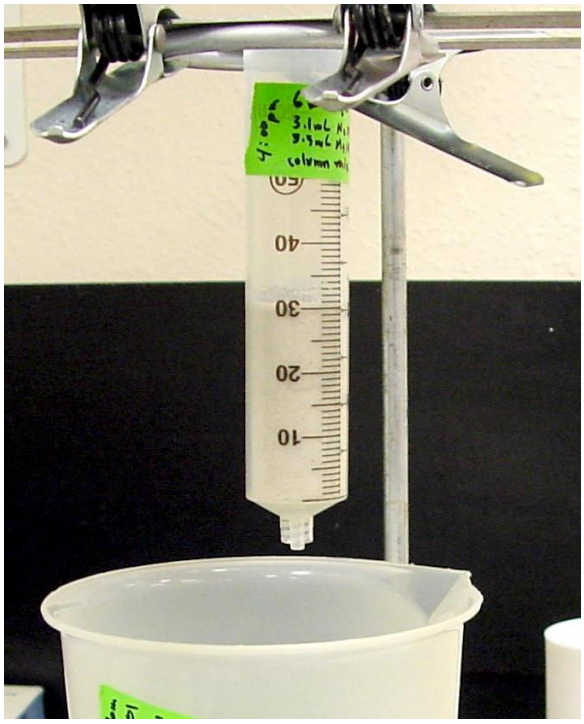


**Figure 4.1** Experimental setup for column mixing experiments and permeability testing. A plastic beaker below the column collects solutions that exit the column.

(Figure 4.1). Mesoporous silicate (MPS) materials and layered double hydroxides (LDH) were deemed the best candidates because these materials have gel characteristics similar to the kaolin group clay gel, but crystallize in a shorter time period appropriate for field application. To enable the precipitate to develop within the pore space of the column *in situ*, the precursor solutions were formed separately. For each material, there were two precursor solutions that after mixing would form a solid precipitate of the desired phase. In the case of the MPS, a third solution, consisting of 1N HCl, was added to lower the pH and maximize the yield.

Permeability after column mixing of the precursor solutions was used to evaluate the potential effectiveness of each precipitate as an in-ground containment and remediation barrier. In the simplest case, fluid permeability can be described by Darcy's law:

$$Q = \left(\frac{kA}{\mu}\right)\left(\frac{\Delta P}{L}\right) \tag{4.1}$$

where $Q$ is the volumetric flow rate of fluid, determined in our experiments by measuring a fixed volume of de-ionized water passing through the sample and recording the time increment in which this takes place. The use of Darcy's law assumes that fluid flow is slow, unidirectional and steady (e.g. *Dullien*, 1992). Of the remaining variables in Eq. 4.1, $A$ is the cross-sectional area of the sample normal to the flow direction and $L$ is the length of the

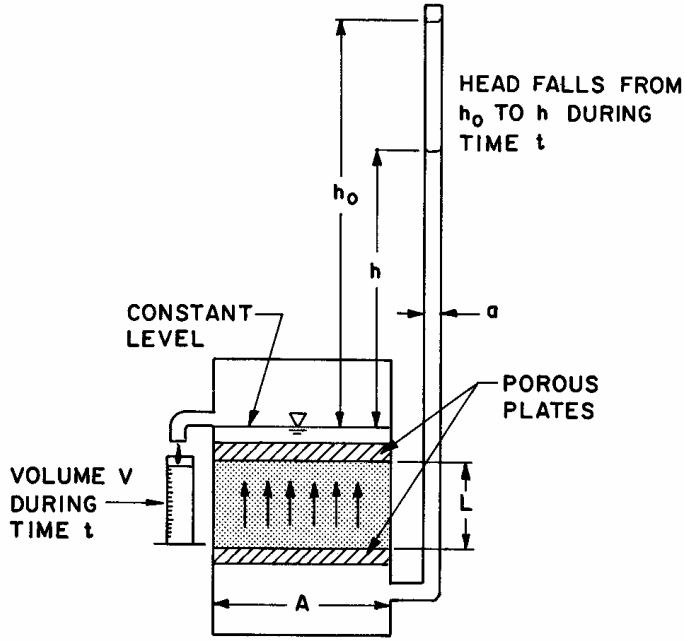


**Figure 4.2** Falling head permeameter testing configuration (after *Dullien*, 1992).

sample in that same direction. $\Delta P$ is the pressure driving the fluid flow and $\mu$ is the viscosity of the fluid, where the constant $k$ is the permeablity of the sample. To determine permeability from the configuration of our laboratory experiment (Figure 4.1) that is similar in design to a falling head permeameter (FHP) test (Figure 4.2), an alternate formulation applies:

$$k = \left( \frac{aL\mu}{At\rho g} \right) \ln(h_0 / h_1) \tag{4.2}$$

Here the symbols are the same as Eq. (1) with the additional terms, $a$ and $t$, being the diameter of the column of water above the sample and the elapsed time, respectively. In our experiments, the diameter of the sample and the diameter of the water column were identical; $a = A$. Specifically, the sample cross-section was $5.38 \times 10^{-6}$ m$^2$ and the flow direction, $L$, was 0.07 m for the 50.00 g of AZ magic sand in our experiments. The driving force for fluid flow is related to the hydrostatic pressure drop, $\Delta P = P_1 - P_2$, measured by the change in the height of the water column, $\Delta h$ (measured from the opening at the bottom of the syringe). With this equation the total elapsed time, $t$, was recorded for a specific height (or volume) of water above the sample, where $h_0$ is the initial height of the fluid in the column at $t_0 = 0$.), and depends linearly on density and gravity as $\rho g \Delta h$, where $\rho = 1000$ kg/m$^3$ and $g = 9.8$ m/s$^2$. The water viscosity, $\mu$, was taken as 0.001 kg/m-s. Thus, Eq. (4.2) reduces to:

$$k = \left( \frac{L\mu}{t\rho g} \right) \ln\left(h_0 / h_1\right) \tag{4.3}$$

Our experimental configuration differs slightly from the example shown in Figure 4.2, because the fluid drains directly at the bottom of the column rather than being directed upwards in a 'U'. However, the change in pressure still behaves as a function of $\rho gh$ and should not affect the measurements provided the fluid flow is slow enough through the sample that continuous flow is maintained between orifices (as was the case).

## 4.1 Experiments to evaluate *in situ* mesoporous silicate precipitation

Seventeen experiments were conducted to evaluate *in situ* precipitation of mesoporous silicate (MPS) in sand packs and the effect on permeability. Experiments were conducted using Arizona Magic Sand, a nearly pure quartz sand of 0.1-1 mm grain size, and U.S. Silica Min-U-Sil-10, a crushed sand with average grain size of 10 microns. The microstructure of the quartz grains are shown in Figure 4.3.

### 4.1.1 Solution preparation and column mixing

Preparation of the mesoporous silicate began by mixing 14.4 g of reagent grade sodium silicate (242.2 g/mol) solution with 30.0 g of de-ionized water. This comprised the first of the two precursor solutions. The second solution was prepared by dissolving 3.3g of hexadecyltrimethylammonium bromide (HDTMA) in 120.0 g of de-ionized water to which the pH had been adjusted to 11.7 by the addition of solid NaOH. Mixing of the sodium silicate solution with the HDTMA solution causes precipitation of the mesoporous silicate. After mixing these solutions, reducing the pH using HCl to a value of 8.5 optimized the amount of precipitation to form from solution.

Equal masses of the large- and small-grained sands were poured into 60 mL and 10 mL syringes, respectively. Sand was held in the syringes using initially a disposable luer-lock filter at the bottom of the syringes. HDTMA solution and Na-silicate solution were added separately to the tops of the columns in proportional amounts calculated to fill, but not exceed, the porosity. Alternate addition of the solutions is necessary to induce the formation of the precipitate within the column, rather than in the mixed solution before it is added to the sediment.

### 4.1.2 Results

Falling head permeability tests were made using deionized water on "columns" with filters removed (Table 4.1). Permeability was calculated as described above, and then converted to hydraulic conductivity. Hydraulic conductivity was reduced 2 to 3 orders of magnitude over that of uncemented quartz columns (from ~7 x $10^{-2}$ cm/sec to 4 x $10^{-5}$ cm/sec), depending on the order of addition of the solutions, air-drying vs. oven-drying at 70º to 75ºC, and the

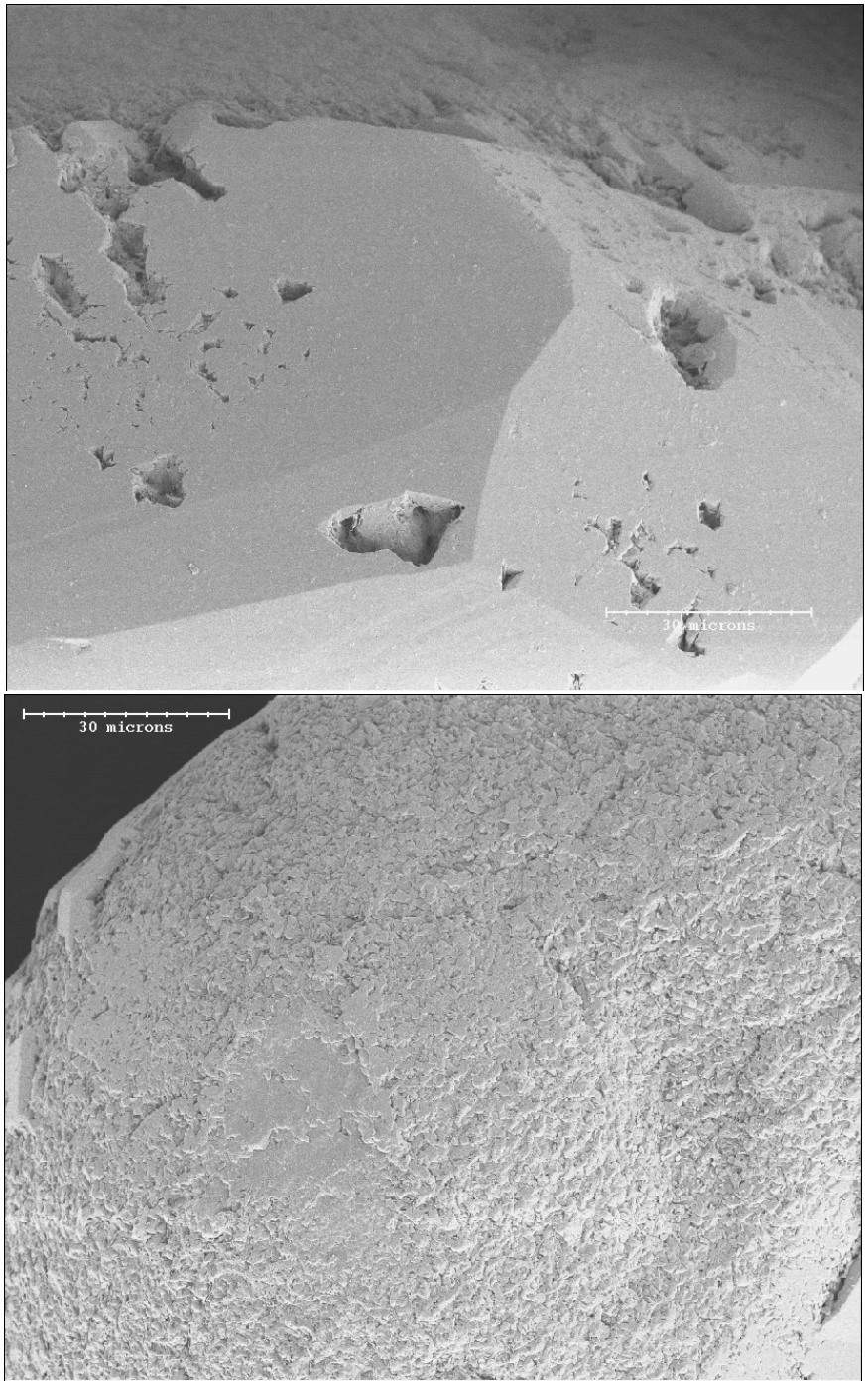


**Figure 4.3** Backscattered electron micrographs showing the bimodal morphology of Arizona magic sand. Grains are smooth and faceted (top), or alternatively rough and irregular (bottom).

number of solution additions (the maximum number was two). In two cases in the oven-dried samples, fluid flow was completely stopped after 3 to 4 days of continuous flow. Generally, flow was faster in all columns when water was first added after the cementing agents had been allowed to dry. Over one to two days, flow would decrease to a steady-state, as represented by the permeability and hydraulic conductivity (Table 4.1).

**Table 4.1** Summary of *in situ* precipitation of mesoporous silicate (MPS) in sand pack experiments.

| Experiment | Quartz (g) | Solutions | Drying Conditions | Darcy permeability ($cm^2$) | Hydraulic conductivity (cm/sec) |
|---|---|---|---|---|---|
| A-10-AZ[1,2] | 2 mL | HDTMA/Na-silicate | 75°C | $1.2 \times 10^{-7}$ | $1.2 \times 10^{-2}$ |
| B-10-AZ[1,2] | 2 mL | Na-silicate/HDTMA | 75°C | $4.8 \times 10^{-9}$ | $4.7 \times 10^{-4}$ |
| 1-60-AZ[3] | 77.53 | Na-silicate/HDTMA x 2 | room T | $5.9 \times 10^{-8}$ | $5.8 \times 10^{-3}$ |
| 2-60-AZ[3,4] | 77.49 | Na-silicate/HDTMA x 2 | 75°C | $4.2 \times 10^{-9}$ | $4.1 \times 10^{-4}$ |
| 3-60-AZ | 77.51 | Na-silicate/HDTMA x 2 | room T | $2.4 \times 10^{-8}$ | $2.3 \times 10^{-3}$ |
| 4-60-AZ[5] | 77.51 | Na-silicate/HDTMA x 2 | room T | $3.9 \times 10^{-8}$ | $3.8 \times 10^{-3}$ |
| 5-60-AZ | 77.51 | HDTMA | room T | rapid flow | rapid flow |
| 6-60-AZ[4] | 77.51 | HDTMA | 70°C | $3.9 \times 10^{-9}$ | $3.8 \times 10^{-4}$ |
| 7-60-AZ | 77.51 | Na-silicate | room T | rapid flow | rapid flow |
| 8-60-AZ | 77.50 | Na-silicate | 70°C | $7.4 \times 10^{-9}$ | $7.2 \times 10^{-4}$ |
| A-10-US[6] | 3.00 | Na-silicate/HDTMA | room T | $4.6 \times 10^{-9}$ | $4.5 \times 10^{-4}$ |
| B-10-US | 3.00 | Na-silicate/HDTMA | room T | $2.5 \times 10^{-9}$ | $2.5 \times 10^{-4}$ |
| C-10-US | 3.00 | Na-silicate/HDTMA | room T | $2.3 \times 10^{-9}$ | $2.3 \times 10^{-4}$ |
| E-10-US | 3.04 | HDTMA | room T | $3.7 \times 10^{-10}$ | $3.7 \times 10^{-5}$ |
| F-10-US | 3.04 | HDTMA | 70°C | $1.4 \times 10^{-9}$ | $1.4 \times 10^{-4}$ |
| G-10-US | 3.04 | Na-silicate | room T | $2.6 \times 10^{-10}$ | $2.5 \times 10^{-5}$ |
| H-10-US | 3.04 | Na-silicate | 70°C | rapid flow | rapid flow |

[1] AZ = Arizona Magic Sand
[2] Mass was not measured in these experiments, but instead quartz sand volume.
[3] Solutions of Na-silicate immediately followed by HDTMA were applied twice, because the volume needed to fill porosity was undercalculated for the first application.
[4] Over one to two days after reported permeability was measured, flow slowed to zero.
[5] Solutions of Na-silicate immediately followed by HDTMA were applied twice, but with a two-day intervening period.
[6] US = U.S. Silica sand.

Generally, flow was faster in all columns when water was first added after the cementing agents had been allowed to dry. Over one to two days, flow would decrease to a steady-state, as represented by the permeability and hydraulic conductivity (Table 4.1).

The sand packs were allowed to sit for ~8 months to assess the integrity of the simulated barrier materials; most samples dried completely during this period as they were not capped tightly with parafilm. In only one experiment was solution flow completely stopped for the 8 months, and that experiment contained only Arizona magic sand and HDTMA (6-60-AZ) (the surfactant used as the templating substrate for MPS materials). All but one of the remaining sand packs dried completely. The sand pack that did not dry completely as well as the sand pack with negligible permeability had both been dried in the oven at 70° to 75°C.

All of the sand packs that contained quartz and precipitated MPS behaved essentially as powders upon complete drying (Figure 4.4). While some quartz would be weakly cemented with mesosilicate precipitate, even this material powdered easily with minimal applied pressure. The only materials that had even slight mechanical integrity were those cemented with Na-silicate solution. If mesoporous silicates are precipitated along with quartz sand as a slurry, the resultant cemented material is slightly more durable and can maintain its integrity (essentially as a plug of material) under small amounts of applied pressure. However, pressing hard against such a plug with a blunt instrument results in the plug breaking apart

**Figure 4.4** Bulk sample following *in situ* precipitation of MPS in sand pack (Arizona magic sand), followed by drying at 60 °C after removal from the column. Indurated material taken from the lower portion of the plastic syringe is located at the left side of the image and mimics the cone shape of the syringe bottom. The larger piece to the right of the image is from the column head where solutions were introduced. The smaller pieces in the center and the loose sand came from space in between the two ends (sample from experiment AZ-MPS-11, Table 4.2).

into smaller pieces. These plugs are not as physically durable as plugs formed by adding Na-silicate only to quartz sand. The microstructure of the samples was evaluated in detail using scanning electron microscopy, presented later in Section 4.3.

The experiments indicated that the *in situ* MPS precipitation under even idealized laboratory conditions failed to achieve one of the key goals which was increased mechanical strength and integrity. While mesoporous silicate did indeed precipitate in the sand packs, the distribution of the precipitate was ineffective in so far as cementing or lithifying the sand pack. For this reason, a second series of experiments was conducted that focused largely on *in situ* precipitation of a layered double hydroxide (similar to naturally occurring hydrotalcite).

## 4.2 Experiments to evaluate *in situ* layered double hydroxide precipitation

Twenty-seven experiments were conducted to evaluate *in situ* precipitation of layered double hydroxide (LDH) in sand packs and the effect on permeability. Experiments were conducted using Arizona Magic Sand, a nearly pure quartz sand of 0.1-1 mm grain size, and U.S. Silica Min-U-Sil-10, a crushed sand with average grain size of 10 microns. A single additional experiment was performed with the mesoporous silicate solution sequence.

### 4.2.1 Solution preparation and column mixing

Similar to the mesoporous silicate synthesis, the LDH synthesis derived from making two separate solutions. The first was an aqueous solution comprised of reagent grade magnesium chloride and aluminum chloride. 40.68 g of $MgCl_2$ and 24.12 g of $AlCl_3$ was added to 300 mL of de-ionized water to produce a 2:1 ratio of magnesium to aluminum. The pH of this solution was 2.5. The second solution was an aqueous solution of 2N sodium hydroxide. When 16.8 mL of the sodium hydroxide solution was added to 18 mL of the salt solution, a milky white precipitate of LDH would form with a pH after mixing of 10.0. Plastic syringes with 60 CC capacity were used as columns to hold the sand packs, that for these experiments consisted solely of Arizona Magic sand. Prior to filling the column with the sand, circles the size of the inner column diameter were cut from high flow rate filter paper (Fisher Brand Q8 #09-790E) and placed at the bottom of the column. The column was suspended over a beaker used to collect effluent from the mixing tests and the aqueous permeant from the permeability tests.

A standard 50.00 g (29 CC) of Arizona Magic sand was used. The volume of pore space in 29 CC of Arizona Magic sand was determined experimentally by water absorption to be approximately 12 CC (yielding a porosity of 41%). The precursor solutions, that after mixing would form the MPS and LDH precipitates, were formulated such that their combined volume would be equal to the estimated pore volume of 12 CC. All solution mixtures were measured and distributed using various pipettes (10-100 μL; 100-1000 μL; 500-5000 μL) that were calibrated with de-ionized water. In general, when fluid was released from the pipette it was done such that the sand at the top of the column was disturbed minimally. After introducing a precursor solution at the top of the column, enough time was allowed for it to be absorbed prior to introducing the next solution. The total amount of time required to introduce the chemicals into the column from the pipette was typically less than 5 minutes for the initial treatment of each precipitate.

Multiple treatments were applied to the sand columns in an effort to maximize the precipitation of solid within the pore space and to subsequently minimize the permeability of the matrix. However, multiple treatments required increasingly longer times between subsequent applications, as the initial permeability reduction would impede the treatment chemicals from diffusing through the column (e.g. - three treatments would take over five hours to complete).

In addition to varying the number of treatments applied to the sand column, other attempts were made to maximize the amount of precipitate. One such approach consisted of varying the order in which the precursor chemicals were introduced into the column. Because solutions with a high pH, such as 2N NaOH, will react strongly with quartz and other minor phases present in the sand, different reactions could possibly occur if these solutions enter the column first, rather than after the complementary solution had already saturated the microstructure. Also, as initial results indicated some effectiveness to the multiple treatments, it was postulated that introducing the precursor solutions into the column in smaller increments might further ensure more adequate mixing and ultimately, greater permeability reduction. The ‘standard’ amount of precursor solution was thus halved so that

**Table 4.2** Summary of *in situ* precipitation of layered double hydroxide (LDH) in sand pack experiments.

| Experiment | Solution (first in column) | No. Treatments | Solution Temperature | Drying Conditions | Measurement Time (s) | Permeability ($m^2$) |
|---|---|---|---|---|---|---|
| 5-U-AZ[1,2] | 2N NaOH | 1x | room T | room T | 5650 | $4.38 \times 10^{-11}$ |
| 7-AZ[1] | Mg/Al (2:1) | 1x | room T | 60 °C | 10630 | $3.65 \times 10^{-12}$ |
| 8-AZ[1] | Mg/Al (2:1) | 1x | room T | room T | 2490 | $6.72 \times 10^{-11}$ |
| 9-AZ[1] | 2N NaOH | 1x | room T | room T | 4320 | $4.45 \times 10^{-11}$ |
| 10-AZ[1] | 2N NaOH | 1x | room T | 60 °C | 2730 | $6.62 \times 10^{-11}$ |
| 11-AZ-MPS[1,3] | Na-Si - 1X | 1x | room T | 60 °C | 9521 | $1.70 \times 10^{-14}$ |
| 13-AZ[1] | 2N NaOH | 1x | room T | room T | 9055 | $3.51 \times 10^{-11}$ |
| 16-AZ[1] | 2N NaOH | 2x | room T | 60 °C | 11580 | $3.65 \times 10^{-12}$ |
| 17-AZ-MPS[1,3] | HDTMA, HCl | 1x | room T | room T | 5423 | $1.48 \times 10^{-14}$ |
| 20-AZ[1] | 2N NaOH | 2x | room T | room T | 15900 | $1.23 \times 10^{-11}$ |
| 21-AZ[1] | Mg/Al (2:1) | 1x | 45 °C | room T | 1350614 | $3.85 \times 10^{-11}$ |
| 22-AZ[1] | 2N NaOH | 2x | 45 °C | room T | 1210476 | $3.51 \times 10^{-11}$ |
| 23-AZ[1] | Mg/Al (2:1) | 2x | 45 °C | room T | 1289005 | $6.71 \times 10^{-12}$ |
| 24-AZ[1] | Mg/Al (2:1) | 2x | room T | room T | 249930 | $4.07 \times 10^{-11}$ |
| 25-AZ[1] | Mg/Al (2:1) | 2x | room T | room T | 149183 | $3.29 \times 10^{-11}$ |
| 26-AZ[1] | Mg/Al (2:1) | 3x | room T | room T | 1013210 | $1.96 \times 10^{-11}$ |
| 27-AZ[1] | Mg/Al (2:1) | 3x | room T | room T | 1270878 | $5.61 \times 10^{-12}$ |
| 28-AZ[1] | Mg/Al (2:1) | 2x | 45 °C | room T | 977270 | $1.73 \times 10^{-11}$ |

[1] AZ = Arizona Magic Sand. All experiments conducted using standard 50.00 g.
[2] U = ultrasonic treatment. Samples immersed in ultrasonic bath for these experiments to enhance mixing.
[3] MPS = mesoporous silicate (rather than LDH) precipitation experiment.

the combined volume was 6 CC, equal to half of the expected pore volume (see Table 4.2). Based on the Phase 1 results, heating of the chemical species was also attempted to increase the efficiency of the precipitate yield. The precursor solutions were placed into small Nalgene containers, sealed with Parafilm and placed into a water bath at 45 °C, for a minimum of 60 minutes. They were quickly removed and pipetted into the column in the same way as the room temperature column mixing experiments. A final technique involved sealing the bottom and end of the column and placing the entire column into an ultrasonic bath for up to 20 minutes, subsequent to applying the precursor chemicals.

### 4.2.2 Results

Falling head permeability tests were made using deionized water on "columns" with filters removed (Table 4.2). Permeability was calculated as described above. Permeability was reduced 1 to 2 orders of magnitude over that of uncemented quartz columns (from ~$2 \times 10^{-9}$ $m^2$ to a minimum of $3 \times 10^{-11}$ $m^2$), depending on the order of addition of the solutions, air-drying vs. oven-drying, and the number of solution additions. Most significantly, heating of the solution as well as increasing the number of chemical treatments causes a decrease in the permeability of the sand packs.

As observed with the previous mesoporous silicate experiments, all of the sand packs that contained quartz and precipitated LDH behaved essentially as powders upon complete drying (Figure 4.5). While some quartz would be weakly cemented with LDH, even this

**Figure 4.5** Bulk sample following *in situ* precipitation of LDH in sand pack (Arizona magic sand), followed by drying at 60 °C after removal from the column. Compared to the experiments with mesoporous silicate precipitation (see Figure 4.4), the indurated regions of the LDH sand packs were smaller and noticeably more friable. Material from the lower region of the column is shown on the left and upper region at the right of the image (sample from experiment AZ-7, Table 4.2).

material powdered easily with minimal applied pressure. The LDH samples were noticeably more friable than the MPS samples.

## 4.3 Microanalysis

Specimens for microanalysis, including high voltage field emission scanning electron microscopy and energy dispersive x-ray spectrometry (EDS), were prepared from both the starting (unreacted) sand, and from both indurated as well as powdered regions of the reacted mesoporous silicate and layered double hydroxide sand packs.

As previously mentioned, Arizona magic is a very pure quartz sand. Scanning electron microscopy (Figure 4.3) reveals a bimodal grain morphology, consisting of grains with faceted, smooth crystalline surfaces and also grains with highly rough and irregular surfaces that are clearly not crystal faces.

The solidified regions of the dried columns appeared to develop similarly for both types of precipitates. Indurated sand particles were found at the head of the column, at the end of the column, and in limited regions within the center of the columns. The pieces taken out of the central regions of the column were smaller in volume as compared to those from the head or bottom of the column, and the extent of induration of the LDH sand packs was generally less

than that for the MPS sand packs. Moreover, the mechanical integrity of the lithified regions within the LDH sand packs was less than that of the MPS sand packs. As discussed below, this may be due to the nature of the precipitate coverage and the inherent strength of the precipitate as discussed below.

The location of the maximum precipitation in the sand packs, associated with indurated regions after drying, suggests the nature of *in situ* mixing within the sand pack. At the top of the sand pack, where the chemicals are introduced by pipette, there may be a region of more thorough mixing that results from kinetic disturbances of the fluid and sand, resulting in increased precipitate yield. Several factors may contribute to an increase in the amount of precipitate formed in the bottom of the sand pack. A funnel effect at the bottom of the sand pack (see Figure 4.1) likely forces unreacted precursor solutions into close proximity, allowing for further mixing. The build up of precipitate and reduction of pore volume at the end of the column could also act to trap or collect solid precipitate that formed higher up in the sand pack, either having been dislodged from a grain surface, or alternatively having precipitated in the pore space without bonding to a grain surface, and traveled through the pore space with the precursor solutions. That precipitate was observed in the effluent indicates unambiguously that precipitate was formed in the pore fluid, rather than nucleating at a grain surface. Finally, pockets of lower permeability material may also have existed randomly throughout the sand pack, allowing for enhanced mixing and subsequently precipitation of solid in random locations.

At low magnifications (Figure 4.6, top), sand grains in an indurated region of the MPS sand pack (from experiment 11-AZ-MPS in Table 4.2) appear unaltered from the original grains in the unreacted sand pack (Figure 4.3). However, high magnification reveals a thin, smooth coating that permeates the grain structure (Figure 4.6, middle). The coating bonds the grains at contact points, forming 'necks' that link grains together (Figure 4.6, bottom). In most cases, the necks (Figure 4.9) show signs of microcracking that could have occurred during either drying or during handling. The lack of widespread occurrence of MPS precipitate in the pore volumes and pore throats is consistent with the observed limited effectiveness in reducing bulk permeability.

In contrast, the LDH sand packs (Figure 4.7) revealed two different precipitate morphologies. Similar to the MPS sand packs, the LDH precipitate coats quartz grains (Figure 4.7); however, the "thickness" of the coating (crystal size) is larger, and platelet particles with typical sizes of 1-3 microns are easily resolved (Figure 4.7). Within the pore network, rose-like platelet structures are found with average platelet sizes approximately 500 nm in dimension (Figure 4.7).

Spectra collected from various locations on both the indurated as well as powdered regions of the MPS and LDH sand packs were in many cases indeterminate, although evidence was found for precipitate formation in some areas (Figures 4.8). The most likely explanation is the small amount of precipitate that formed within the MPS sand packs, and the ultrafine crystalline nature of the LDH precipitate (as observed in the LDH sandpacks), could not provide a sufficiently strong x-ray signal that could be distinguished from the very strong Si peak of the underlying quartz grains.

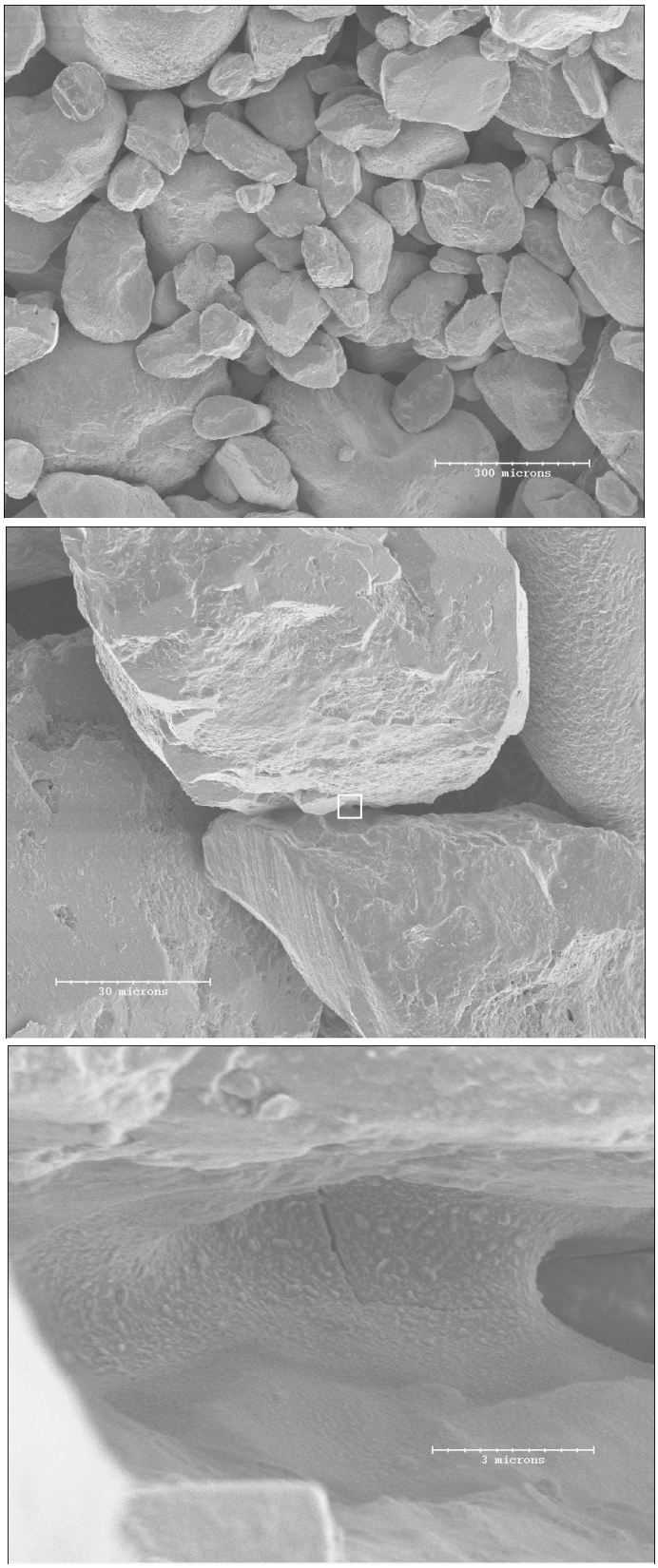


**Figure 4.6** (Top) A low magnification back scattered electron micrograph of an indurated region of a MPS sand pack after drying at 60 °C. The sand pack appears unchanged from the starting material, and the cohesion following the experiment suggests the presence of a very thin coating of MPS precipitate. (Middle) A "neck" of MPS precipitate can be observed between two sand grains (boxed region). (Bottom) A higher magnification view of the MPS precipitate bridging the two grains shown in the middle micrograph. (Sample from experiment AZ-MPS-11.)

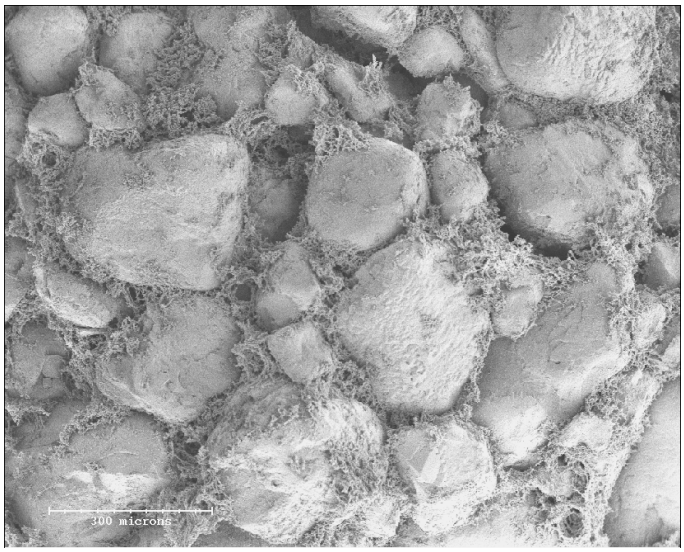


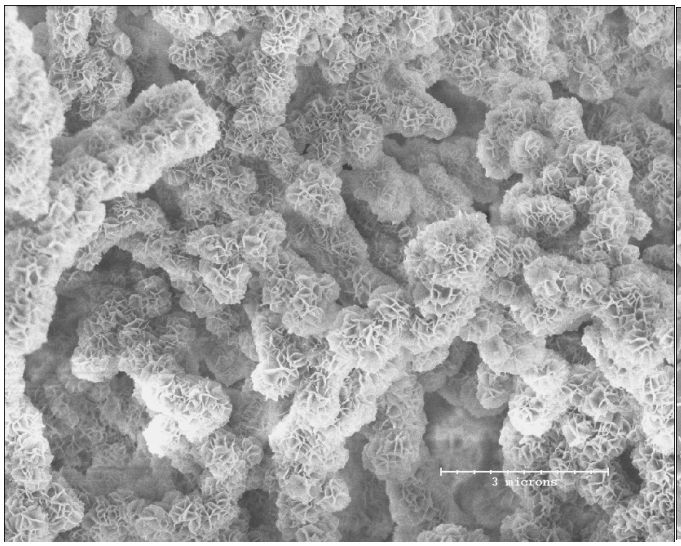


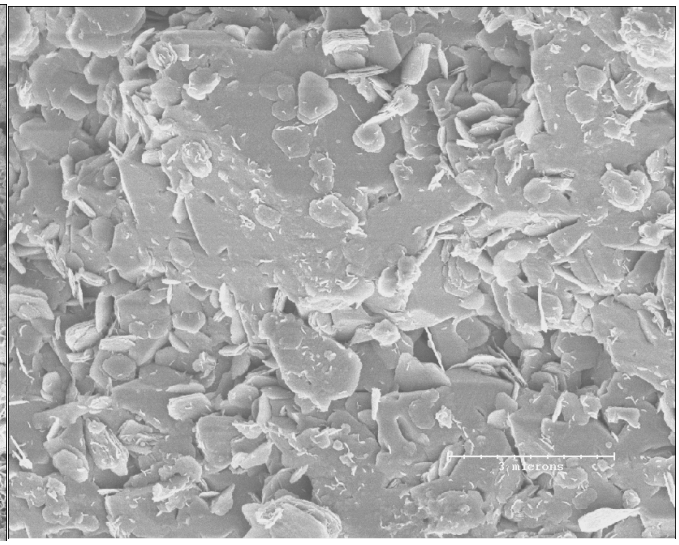


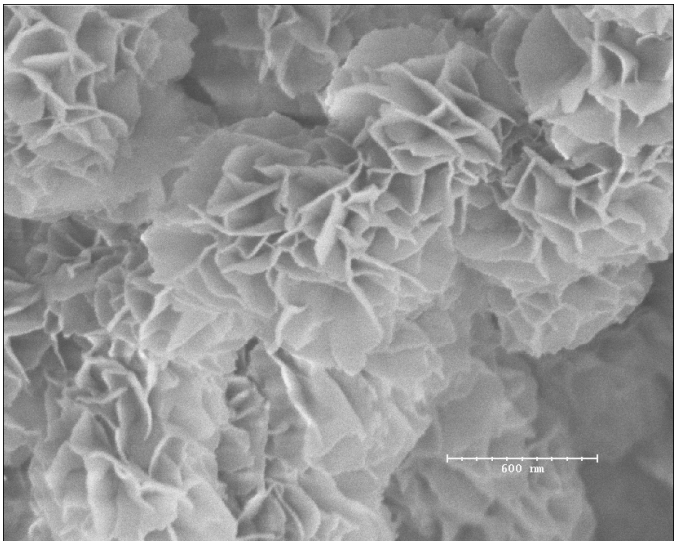


**Figure 4.7** (Top) A low magnification back scattered electron micrograph of an indurated region of an LDH sand pack after drying at 60 °C. (Middle) The LDH precipitate is clearly evident as a coating over grains (right) where platelet size is a few microns, and partially filling the pore space where sub-micron platelets dominate (left). Despite the pervasiveness of the coating, the strength of the bonded LDH sand packs is less than that of the MPS sand packs. (Lower) The rose-like morphology of the LDH precipitate partially filling previously open pore space (left middle) is very well developed. The typical size of the platelets is 500 nm. (Sample from experiment AZ-7.)

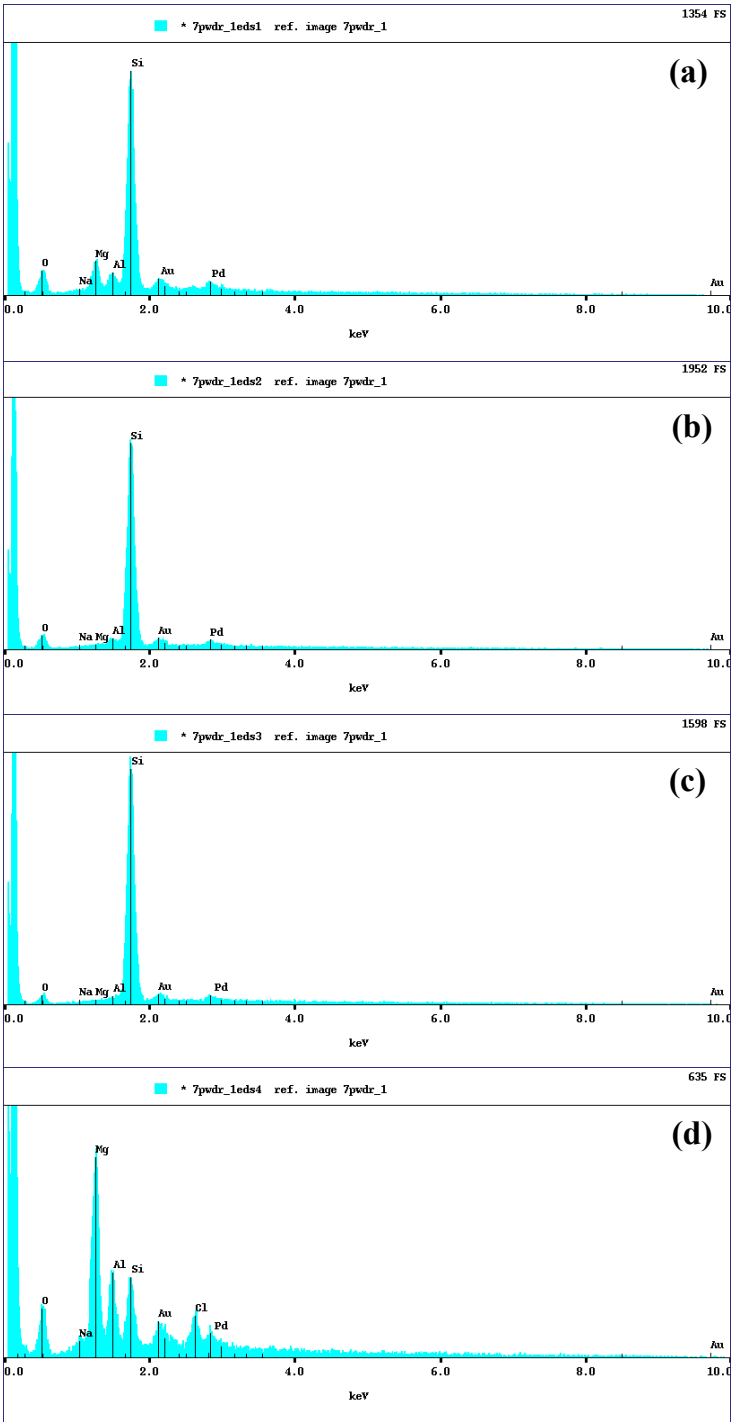


**Figure 4.8** Spectra collected from powdered region from LDH precipitation experiment AZ-7. A light gold-palladium film coats all samples as required in scanning electron microscopy. (Top) The signal for Mg and Al is moderate as are the Au-Pd peaks. (Middle) The Mg/Al signal from these two regions is minimal, indicating possible lack of coverage or incomplete formation of LDH. (Bottom) The signal here is strong and in the proper ratio (2:1) of the precursor solutions. The presence of the chlorine peak suggests that this area contains remnants of the unreacted precursor solution.

# 5 Summary

The purpose of project CU-1093 "In-Situ Clay Formation: A New Technology for Stable Containment Barriers" was to establish the viability of a proposed new type of containment barrier, derived from the in situ precipitation of clays in the pore space of contaminated soils or sediments, with a potentially broad range of environmental stability and longevity.

The Phase 1 effort focused on the laboratory synthesis of clays and clay-like materials from gels at room or ambient temperature, with promising results (*Manceau et al*., 1999; *Zhao et al*., 2000, *Zhao et al*., in press). The Phase 2 effort focused on precipitation of the two most promising clay or clay-like materials identified in Phase 1, mesoporous silica and layered double hydroxide, in natural sediments under laboratory conditions. Success of the method was to be demonstrated by obtaining a significant reduction in hydraulic conductivity and increase in geomechanical stability, under conditions practical for field application. The experiments needed to demonstrate that practical quantities of clays and/or clay-like solids could be formed within a timeframe appropriate for installment of a barrier, and secondly, that the material properties would be improved over those of existing containment barriers.

While some success was achieved in the Phase 2 effort, the laboratory experiments failed to achieve one of the key goals, increased mechanical stability. Further, engineering and environmental considerations were envisioned to complicate field-scale implementation of the process. The ultra-high acidic and basic pH of the precursor chemicals would require non-standard materials to hold, ship, and inject into the ground environment. Moreover, at these same pH levels, the precursor materials might be considered as damaging, if not more so, than some of the contamination plumes they were sought to control. Finally, the mesoporous silicate and layered double hydroxide clay-like materials were not likely to remain stable in the in situ environment for long (due to the near-neutral pH of the natural environment), which again violated one of the central premises for the research. The combination of these factors, combined with the observed level of permeability reduction indicates that the systems investigated, while scientifically interesting, are not likely to lead to a viable method to mitigate contaminated ground wastes.

# 6 References


Dullien, F.A.L., Porous *Media – Fluid Transport and Pore Structure*, 2nd ed., Academic Press, New York, New York, 1992.

Anderson M. T., J. E. Martin, J. Odinek, and P. Newcomer (1995) Synthesis of surfactant - templated mesoporous materials from homogeneous solutions. In T. J. Pinnavaia and M. F. Thorpe (ed.) *Access in Nanoporous Materials*, Plenum Press, New York, 29-37.

Borling D., Chan K., Hughes T., and Sydansk R. (1994) Pushing out the oil with conformance control. *Oilfield Review* 6, 44-58.

Bowman R. S., Haggerty G. M., Huddleston R. G., Neel D., and Flynn M. (1995) Sorption of nonpolar organics, inorganic cations, and inorganic anions by surfactant-modified zeolites. In D. A. Sabatini, R. C. Knox, and J. H. Harwell (eds.). *Surfactant-enhanced remediation of subsurface contamination*, ACS Symp. Ser. 594, ACS, 54-64.

Cavani F., F. Trifiro, and A. Vaccari (1991) Hydrotalcite-type anionic clays: preparation, properties and applications. *Catalysis Today* 11, 173-301.

Davidovits J. (1993) New confinement concepts based on geopolymeric materials. In Geoconfine 93, *Proc. Int. Symp*. M. Arnould, M. Barres, and B. Come (eds.). A. A. Balkema, Rotterdam, 499-504.

Decarreau A. (1980) Cristallogène Cristallogène des smectites magnésiennes: hectorite, stévensite. *Bull. Mineral*. 103, 579-590.

Decarreau A. (1981) Cristallogenèse à basse température de smectites trioctaédriques par vieillissement de coprécipités silicométalliques de formule $(Si_{4-x})M_3^{2+}O_{11}\bullet nH_2O$, où x varie de 0 à 1 et où $M^{2+}$ = Mg-Ni-Co-Zn-Fe-Cu-Mn. C. R. *Acad. Sci. Paris* 292, 61-64.

Decarreau A. and D. Bonnin D. (1986) Synthesis and crystallogenesis at low temperature of Fe(Ul)-smectites by evolution of coprecipitated gels: experiments in partially reducing conditions. *Clay Min*. 21, 861-877.

Decarreau A., D. Bonnin, D. Badaut-Trauth, R. Couty, and P. Kaiser (1987) Synthesis and crysulogenesis of ferric smectite by evolution of Si-Fe coprecipitates in oxidizing conditions. *Clay Min.* 22, 207-223.

Environmental Protection Agency (1995) In-situ remediation technology status report. Treatment Wells. Report EPA A542-K-94-004, 12-25.

Evans J. C. (1996) Soil- and cement-based vertical barriers with focus on materials. Chapter 2 in *Assessment of Barrier Containment Technologies: A Comprehensive Treatment for Environmental Remediation Applications*, Rumer R. R. and Mitchell J. K. (eds.), 5-43.

Flehmig W. (I 992) The synthesis of 2M I -illitic micas at 20'C. N. Jb. Miner. Mh. H. I 1, 507-512.

Filz G. M. and Mitchell J. K. (1996) Design, construction, and performance of soil- and cement-based vertical barriers. Chapter 3 in *Assessment of Barrier Containment Technologies: A Comprehensive Treatment for Environmental Remediation Applications*, Rumer R. R. and Mitchell J. K. (eds.), 45-75.

Harder H. (1971) The role of magnesium in the formation of smectite minerals. *Chem. Geol*. 10,31-39.

Harder H. (1974) Ulite mineral synthesis at surface temperatures. *Chem. Geol*. 14, 241-253.

Harder H. (1976) Nontronite synthesis at low temperatures. *Chem. Geol*. 18, 169-180.

Harder H. (1977) Clay mineral formation under lateritic weathering conditions. *Clay Min*. 12, 281-288.

Harder H. (1978) Synthesis of iron layer silicate minerals under natural conditions. *Clay Min.* 26, 65-72.

Hem J. D. and Lind C. J. (I 974) Kaolinite synthesis at 25C. *Science* 184, 1171-1173.

Johnston C. T. (1996) Sorption of organic compounds on clay minerals: a surface functional group approach. In *Organic Pollutants in the Environment*, Vol. 8, Clay Min. Soc. Workshop Lectures, 2-44.

Kresge, C. T., M. E. Leonowicz, W. J. Roth, J. C. Vartuli, and J. S. Beck (1992) Ordered mesoporous molecular sieves synthesized by a liquid-crystal templating mechanism. *Nature* 359, 710-712.

La Iglesia Fernandez, A. and J. L. Martin Vivaldi (1973) A contribution to the synthesis of kaolinite. *Proc. Int. Clay Conf.* 1972, J. M. Serratosa (ed.),Division de Ciencias C.S.I.C., Madrid, 173-185.

La Iglesia A. and J. L. Martfn-Vivaldi (1975) Synthesis of kaolinite by homogeneous precipitation at room temperature 1. Use of anionic resins in (OH) form. *Clay Min*. 10, 399-405.

La Iglesia A. and J. Sema (1974) Cristalizaci6n de caolinita por precipitaci6n homogenea. Parte11. Empleo de resinas cati6nicas en fase H+. Estud. *Geol. Madrid* 30, 281-287.

Linares J. and F. Huertas (1971a) Kaolinite: synthesis at room temperature. *Nature* 171, 896-897.

Linares J. and F. Huertas (1997b) Sintesis de minerales a temperature ordinaria 1. Estudio preliminar. *Boletin Geologico y Minero* T. LXXXII-1, 77-86.

Manceau A., Schlegel M., Nagy K. L., and Charlet L. (1999) Evidence for the formation of trioctahedral clay upon sorption of Co 2+ on quartz, *J. Coll. Inter. Sci*. 220, 181-197.

McCullen S. B., J. C. Vartuli, C. T. Kresge, W. J. Roth, J. S. Beck, K. D. Schmitt, M. E.Leonowicz, J. L. Schlenker, S. S. Shih and J. D. Lutner (1995) A new family of mesoporous molecular sieves. In *Access in Nanoporous Materials*, T. J. Pinnavaia and M. F. Thorpe,(eds.). Plenum Press, New York, 1-11.

Michalopoulos P. and Aller R. C. (1995) Rapid clay mineral formation in Amazon Delta sediments: Reverse weathering and oceanic elemental cycles. *Science* 270, 614-617.

Parker A. and Davidson C. (1989) Process for retarding and controlling the formation of gel. United States Patent 4,889,563. Dec. 26, 1989.

Raussell-Colom J. A. and Serratosa J. M. (1987) Reactions of clays with organic substances. In *Chemistry of Clays and Clay Minerals*, Newman A.C.D. (ed.), Wiley & Sons, New York., p. 371-324.

Rumer R. R. and Ryan M. E. (eds.) (1995) *Barrier Containment Technologies for Environmental Remediation Applications*. John Wiley & Sons, Inc., New York, 170 p.

Shoemaker S. H., J. F. Greiner, and R. W. Gillham (1996) *Permeable reactive barriers. Chapter II in Assessment of Barrier Containment Technologies: A Comprehensive Treatment for Environmental Remediation Applications*, Rumer R. R. and Mitchell J. K. (eds.), 301-353.

Siffert B. (1962) Quelques reactions de la silice en solution: la formation des argiles. *Memoiresdu Service de al carte geologique d'Alsace et de Lorraine* 21, 86 p.

Siffert B. and R. Wey (1973) Contribution a la connaissance de la synthese des kaolins. *Proc. Int. Clay Conf.* 1972 (J. M. Serratosa, ed.), Division de Ciencias C.S.I.C., Madrid, 159-171.

Taylor R. M., and R. M. McKenzie (1980) The influence of Al on iron oxides. VI. The formation of Fe(Il)-Al (111) hydroxy-chlorides, -sulphates and -carbonates as new members of the pyrozurite group and their possible significance in soils. *Clay Miner*. 28, 179-187.

Whang J. M. (1996) Chemical-based barrier materials, Chapter 9 in *Assessment of Barrier Containment Technologies: A Comprehensive Treatment for Environmental Remediation Applications*, Rumer R. R. and Ryan M. E. (eds.), 211-246.

Zhao H. T., Nagy K. L., Wapies J. S., and Vance G. F. (2000) Surfactant-templated mesoporous silicate materials as sorbents for organic pollutants in water. *Environ. Sci. Technol.* 2000, 4822-4827.

Zhao H. and Nagy K. L., Dodecyl-sulfate-grafted hydrotalcite-like nanocomposites for trapping chlorinated organic pollutants in water, *J. Coll. Inter. Sci.* (in press).

External Distribution:

Dr. Andrea Leeson
SERDP/ESTP Program Office
901 North Stuart St.
Suite 303
Arlington, VA 22203

Mr. Scott Dockum (3)
SERDP Program Support Office
HydroGeoLogic, Inc.
1155 Herndon Parkway, Suite 900
Herndon, VA 20170

Professor K. L. Nagy
Department of Earth and Environmental Sciences
University of Illinois at Chicago (MC-186)
845 West Taylor Street
Chicago, IL 60607-7059

Dr. Anthony A. DiGiovanni
Technology Assessment & Transfer
133 Defense Hwy., #212
Annapolis, MD 21401

Internal Distribution:

MS0750 J. T. Fredrich, 6116 (3)
MS0750 G. J. Elbring, 6116
MS0706 D. J. Borns, 6113
MS0735 R. Finley, 6115
MS0751 L. S. Costin, 6117
MS0750 T. Hinkebein, 6118
MS0710 J. Merson, 6100
MS9018 Central Technical Files, 8945-1
MS0899 Technical Library, 9616 (2)